ISSN 1674-1056
http://cpb.iphy.ac.cn
http://iopscience.iop.org/cpb
中国物理 B
Chinese Physics
中国物理 Chinese Physics B

Influences of adsorptions of some inorganic molecules on electronic, optical, and thermodynamic properties of $Mg_{12}O_{12}$ nanocage: A computational approach

Asghar Mohammadi Hesari, Hamid Reza Shamlouei

Citation: Chin. Phys. B . 2018, 27(8): 084210. **doi:** 10.1088/1674-1056/27/8/084210

Journal homepage: http://cpb.iphy.ac.cn; http://iopscience.iop.org/cpb

What follows is a list of articles you may be interested in

MoS_2 saturable absorber prepared by chemical vapor deposition method for nonlinear control in Q-switching fiber laser

Meng-Li Liu(刘孟丽), Yu-Yi OuYang(欧阳毓一), Huan-Ran Hou(侯焕然), Ming Lei(雷鸣), Wen-Jun Liu(刘文军), Zhi-Yi Wei(魏志义)

Chin. Phys. B . 2018, 27(8): 084211. **doi:** 10.1088/1674-1056/27/8/084211

Structural, vibrational, optical, photoluminescence, thermal, dielectric, and mechanical studies on zinc (tris) thiourea sulfate single crystal: A noticeable effect of organic dye

Mohd Shkir, V Ganesh, S AlFaify, I S Yahia, Mohd Anis

Chin. Phys. B . 2018, 27(5): 054216. **doi:** 10.1088/1674-1056/27/5/054216

Influence of alkali metal superoxides on structure, electronic, and optical properties of $Be_{12}O_{12}$nanocage: Density functional theory study

Ali Raoof Toosi, Hamid Reza Shamlouei, Asghar Mohammadi Hesari

Chin. Phys. B . 2016, 25(9): 094220. **doi:** 10.1088/1674-1056/25/9/094220

First-principles study of structure and nonlinear optical properties of $CdHg(SCN)_4$ crystal

Zhang Peng, Kong Chui-Gang, Zheng Chao, Wang Xin-Qiang, Ma Yue, Feng Jin-Bo, Jiao Yu-Qiu, Lu Gui-Wu

Chin. Phys. B . 2015, 24(2): 024221. **doi:** 10.1088/1674-1056/24/2/024221

Rectification effect in asymmetric Kerr nonlinear medium

Liu Wan-Guo, Pan Feng-Ming, Cai Li-Wei

Chin. Phys. B . 2014, 23(6): 064213. **doi:** 10.1088/1674-1056/23/6/064213

Influences of adsorptions of some inorganic molecules on electronic, optical, and thermodynamic properties of $Mg_{12}O_{12}$ nanocage: A computational approach

Asghar Mohammadi Hesari and Hamid Reza Shamlouei†

Chemistry Department, Lorestan University, Khorram Abad, Lorestan, Iran

(Received 2 February 2018; revised manuscript received 14 March 2018; published online 10 July 2018)

According to density functional theory, we investigate the effects of BF_3, BF_4, BCl_3, AlF_3, $AlCl_3$, $AlBr_3$, BeF_3, GaF_3, $GaCl_3$, $GaBr_3$, NO_3, BS_2, BSO, BO_2, F_2, PF_5, PCl_5, and ASF_5 molecules on the geometric, electronic, linear, and nonlinear optical properties of an $Mg_{12}O_{12}$ nanocage. The thermodynamic stability and feasibility of the adsorption process are investigated by analyzing the free energy. It is shown that the adsorptions of almost all molecules on the $Mg_{12}O_{12}$ surface are exothermic. The calculations of the polarizability of these nanoclusters show that among the studied molecules, BeF_3 has the largest influence on the polarizability value ($\alpha \approx 315$ a.u., the unit a.u. is short for atomic unit). The static first hyperpolarizability (β_0) value is increased in the presence of these superhalogens. This increase is greatest for BeF_3 and BF_4 of which the highest value of the first hyperpolarizability ($\beta_0 \approx 5775$ a.u.) is related to a BeF_3_c(e@$Mg_{12}O_{12}$) nanocluster. The adsorption position is a key to estimating the value of increasing the first hyperpolarizability.

Keywords: $Mg_{12}O_{12}$, polarizability, hyperpolarizability, binding energy, nanocage, DFT calculation

PACS: 42.70.Mp **DOI:** 10.1088/1674-1056/27/8/084210

1. Introduction

Nonlinear optics (NLO) is a branch of optics that describes the nonlinear relationship between dielectric polarization P and electric field E. Nonlinear optical materials have been the subject of broad research in the past few decades because of their potential applications in technological applications such as optical switching, signal processing, information storage, optical communication, laser technology, and chemical and biological species detection.[1,2]

The systematic study of the NLO properties really become possible since the invention of the laser. The first nonlinear optical laser experiment was performed by Franken *et al.* by using a ruby laser. They discovered the second harmonic generation (SHG), in which nonlinear optical material mediates the adding-up of two photons with the same frequency to form a new photon with twice the frequency.[3] The NLO susceptibility $\chi^{(2)}$ describes the SHG process. The $\chi^{(2)}$ is a third-rank tensor with 27 components and is related to the first hyperpolarizability β of a molecule.

In recent decades extensive studies have been conducted to develop new compounds with high NLO response and meet the technological requirements for various applications.[4–14]

In our previous research, we found that the alkali metal oxide adsorption on a $Mg_{12}O_{12}$ nanocage leads to a huge static first hyperpolarizability.[15] In another work, we showed that the first hyperpolarizability value increases by substituting a magnesium atom of a $Mg_{12}O_{12}$ nanocage with a transition metal atom.[16] The influences of Sc doping on the optical properties of $Be_{12}O_{12}$, $Mg_{12}O_{12}$, and $Ca_{12}O_{12}$ nanocages were investigated.[17] The effects of superalkalis M_3O (M = Li, Na, and K) on the nonlinear optical properties of C_{20} fullerene nanoclusters[18] and $Be_{12}O_{12}$ nanocage[19] have been studied.

In this paper, we theoretically study the effects of adsorbing some inorganic molecules on structures, energetic, electronic, thermodynamic, and the linear and nonlinear optical properties of an $Mg_{12}O_{12}$ nanocage.

2. Computational details

Structural optimizations for the ground state of an $Mg_{12}O_{12}$ nanocage and XY_n(e@Mg12O12; (XY_n = BF_3, BF_4, BCl_3, AlF_3, $AlCl_3$, $AlBr_3$, BeF_3, GaF_3, $GaCl_3$, $GaBr_3$, NO_3, BS_2, BSO, BO_2, F_2, PF_5, and PCl_5, ASF_5) were performed by using the density functional method, the unrestricted B3LYP,[20,21] and 6-31+G(d) basis sets. All the calculations converged to an optimized geometry, which corresponds to a true energy minimum as revealed by the lack of imaginary values in the calculated vibration frequencies. Vibration frequencies are calculated at the same level. All the structural optimizations were performed without any symmetry constraints with the Gaussian 09 package.[22] A Gauss-Sum program has been used to calculate the electronic den-

†Corresponding author. E-mail: shamlouei.ha@lu.ac.ir

© 2018 Chinese Physical Society and IOP Publishing Ltd

sity of states (DOS). The energy gap (E_g) that refers to the energy difference between the highest occupied molecular orbital (HOMO) and the lowest unoccupied molecular orbital (LUMO) was calculated from the density of states.

The coulomb-attenuating hybrid exchange-correlation functional method (CAM-B3LYP) with 6-31+G(d) basis sets was used to calculate the dipole moment, polarizability, and first hyperpolarizability.[23] A natural bond orbital (NBO) charge analysis was performed at the same level for all optimized structures.

In a constant and weak electric field the total energy of the system can be expressed as follows:[24,25]

$$E = E^0 - \mu_\alpha^0 F_\alpha - \frac{1}{2}\beta_{\alpha\beta\gamma}F_\alpha F_\beta F_{g\gamma} - \frac{1}{24}\beta_{\alpha\beta\gamma}F_\alpha F_\beta F_{g\gamma}F_\delta = \cdots. \quad (1)$$

Here, E^0 is the molecular energy of the system in the absence of an electric field and F_α is the electric field component along the α direction, μ_α^0 is the permanent dipole moment, $\alpha_{\alpha\beta}$ is the static dipole polarizability (linear polarizability), $\beta_{\alpha\beta\gamma}$ and $\gamma_{\alpha\beta\gamma\delta}$ are the first and second hyperpolarizabilities respectively, with indices α, β, γ, δ, ... referring to the Einstein summation of distinct tensor components.

The definitions of the total dipole moment (μ), mean polarizability (α), and magnitude of static first hyperpolarizability (β_0) are as follows:[5,26,27]

$$\mu = (\mu_x^2 + \mu_y^2 + \mu_z^2)^{1/2}, \quad (2)$$

$$\alpha = \frac{1}{3}(\alpha_{xx} + \alpha_{yy} + \alpha_{zz}), \quad (3)$$

$$\beta_0 = \left[(\beta_{xxx} + \beta_{xyy} + \beta_{xzz})^2 + (\beta_{yyy} + \beta_{yxx} + \beta_{yzz})^2 + (\beta_{zzz} + \beta_{zxx} + \beta_{zyy})^2\right]^{1/2}. \quad (4)$$

3. Results and discussion

3.1. Geometric structure and thermodynamic properties

The optimized ground-state geometry of $Mg_{12}O_{12}$ is shown in Fig. 1, and the selected bond lengths and bond angles are also depicted in Fig. 1.

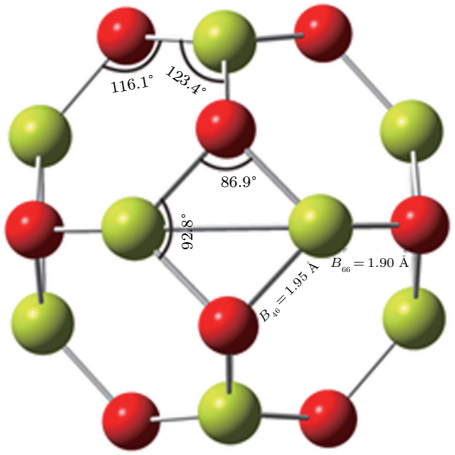
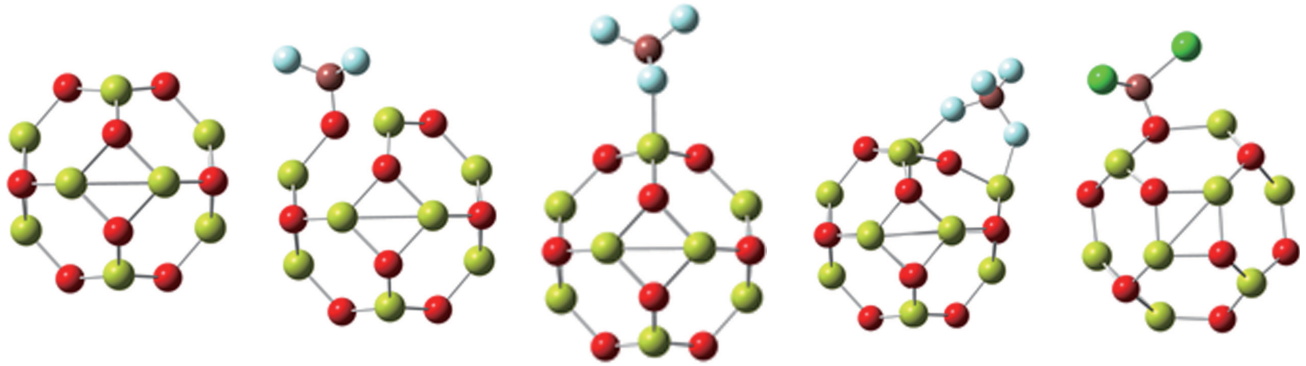


Fig. 1. (color online) Optimized ground-state geometries of $Mg_{12}O_{12}$. In the figure, and represent O and Mg, respectively.

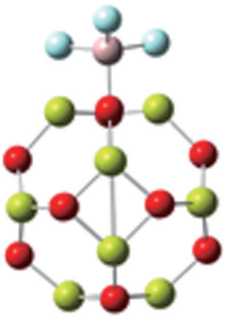
An $Mg_{12}O_{12}$ nanocage is formed from eight 6-member (6-MR) rings and six 4-member (4-MR) rings. There are two distinct Mg–O bonds in the $Mg_{12}O_{12}$ nanocage, one is shared by two 6-MR rings (B_{66}) and the other by a 4-MR ring and a 6-MR ring (B_{46}) where their lengths are 1.90 Å and 1.95 Å respectively, which is compatible with previous results.[16,28]

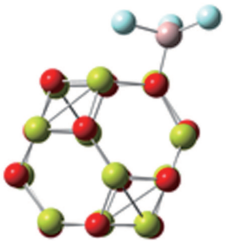
The optimized ground-state geometries for $XY_n(e@Mg_{12}O_{12})$ where $XY_n = BF_3$, BF_4, BCl_3, AlF_3, $AlCl_3$, $AlBr_3$, BeF_3, GaF_3, $GaCl_3$, $GaBr_3$, NO_3, BS_2, BSO, BO_2, F_2, PF_5, PCl_5, and ASF_5 are shown in Fig. 2.

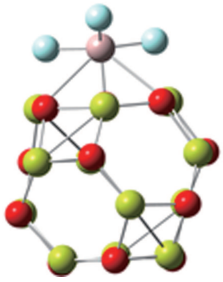
In order to determine the thermodynamic feasibility of the adsorption process, the changes of Gibbs free energy (ΔG^0), the entropy ΔS^0, and the enthalpy (ΔH^0) are all obtained at standard temperature and pressure (1.0 atmosphere and 298.15 K) from the vibrational frequency calculation results. The ΔG^0 is the fundamental criterion to determine whether a process occurs spontaneously. For a given temperature, a process is considered to be spontaneous if the ΔG^0 has a negative value. Moreover, if ΔH^0 is positive, the process is endothermic and if it is negative, the process is exothermic. These results are presented in Table 1.

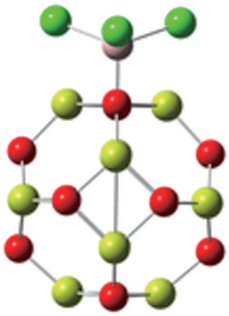


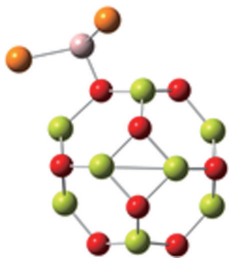
$Mg_{12}O_{12}$ $BF_{3-}a(e@Mg_{12}O_{12})$ $BF_{4-}a(e@Mg_{12}O_{12})$ $BF_{4-}b(e@Mg_{12}O_{12})$ $BCl_{3-}b(e@Mg_{12}O_{12})$

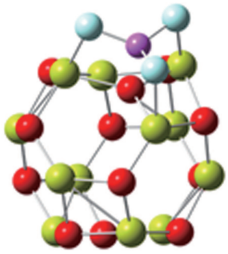

$AlF_{3-}a(e@Mg_{12}O_{12})$

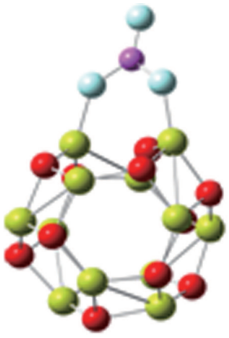

$AlF_{3-}b(e@Mg_{12}O_{12})$

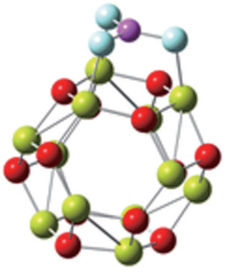

$AlF_{3-}c(e@Mg_{12}O_{12})$

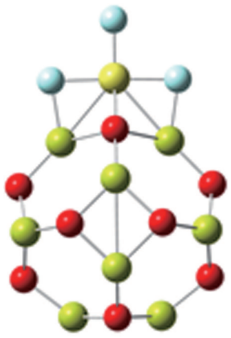

$AlCl_{3-}b(e@Mg_{12}O_{12})$

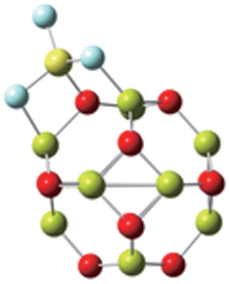

$AlBr_{3-}b(e@Mg_{12}O_{12})$

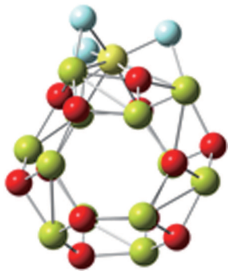

$BeF_{3-}a(e@Mg_{12}O_{12})$

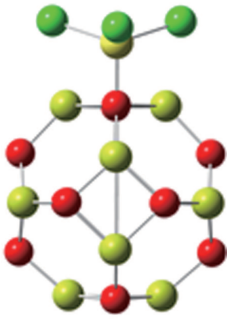

$BeF_{3-}b(e@Mg_{12}O_{12})$

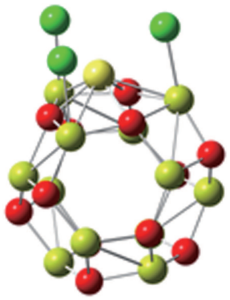

$BeF_{3-}c(e@Mg_{12}O_{12})$

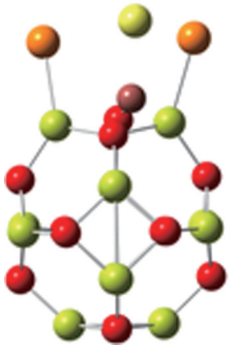

$GaF_{3-}a(e@Mg_{12}O_{12})$

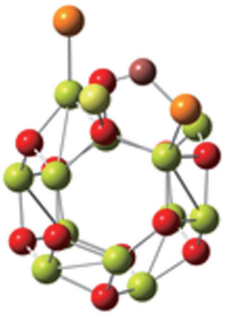

$GaF_{3-}b(e@Mg_{12}O_{12})$

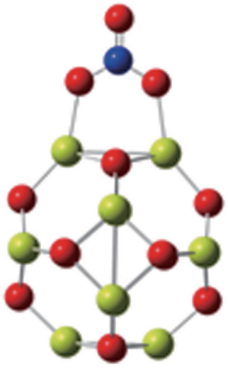

$GaF_{3-}c(e@Mg_{12}O_{12})$

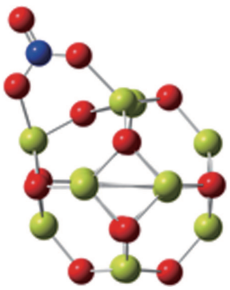

$GaCl_{3-}b(e@Mg_{12}O_{12})$

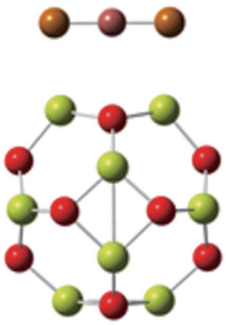

$GaCl_{3-}c(e@Mg_{12}O_{12})$

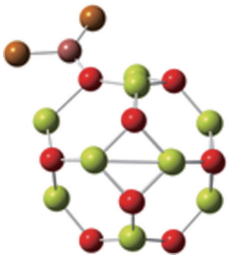

$GaBr_{3-}a(e@Mg_{12}O_{12})$

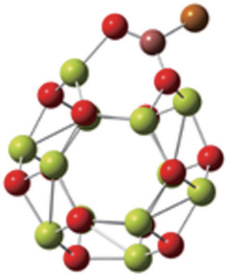

$GaBr_{3-}b(e@Mg_{12}O_{12})$

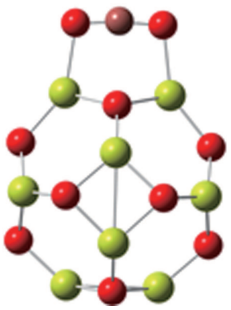

$NO_{3-}b(e@Mg_{12}O_{12})$

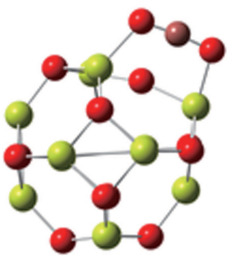

$NO_{3-}c(e@Mg_{12}O_{12})$

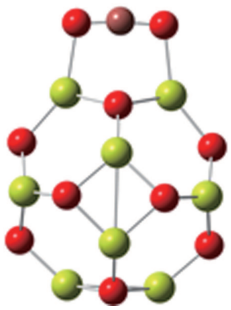

$BS_{2-}a(e@Mg_{12}O_{12})$

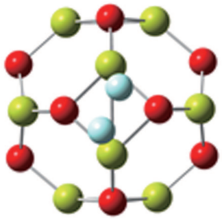

$BS_{2-}b(e@Mg_{12}O_{12})$

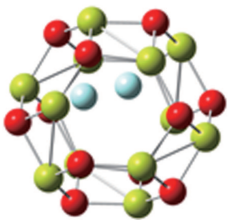

$BSO_{2-}a(e@Mg_{12}O_{12})$


$BO_{2-}a(e@Mg_{12}O_{12})$


$BO_{2-}b(e@Mg_{12}O_{12})$


$BO_{2-}c(e@Mg_{12}O_{12})$


$F_{2-}a(e@Mg_{12}O_{12})$


$F_{2-}b(e@Mg_{12}O_{12})$

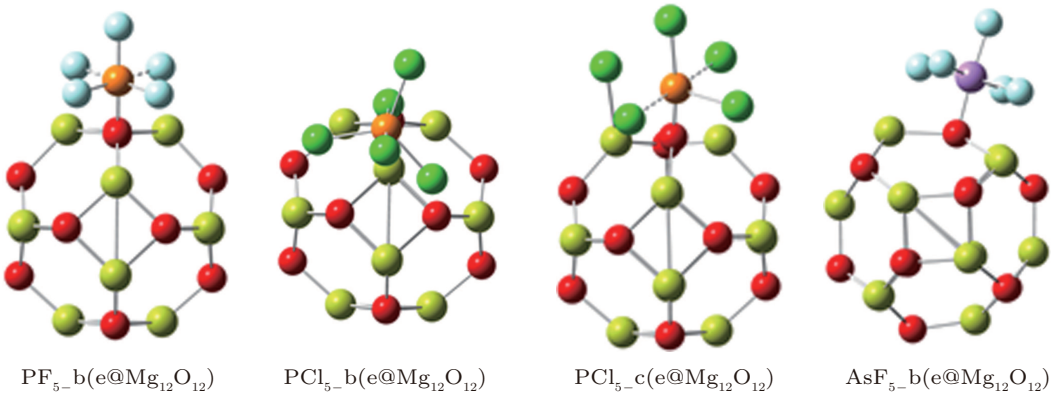


Fig. 2. (color online) Optimized ground-state geometries of $Mg_{12}O_{12}$ and, $XY_n(e@Mg_{12}O_{12})$ (XY_n = BF_3, BF_4, BCl_3, AlF_3, $AlCl_3$, $AlBr_3$, BeF_3, GaF_3, $GaCl_3$, $GaBr_3$, NO_3, BS_2, BSO, BO_2, F_2, PF_5, PCl_5, ASF_5). , , , , , , , , , , and represent the O, Mg, B, F, Cl, Al, Be, Ga, N, P, and As atoms, respectively.

The results of Table 1 show that ΔG^0 values are all negative except for F_2_a(e@$Mg_{12}O_{12}$), F_2_b(e@$Mg_{12}O_{12}$), and PCl_5_b(e@$Mg_{12}O_{12}$). The negative value of ΔG^0 indicates the feasibility and spontaneous nature of the adsorption process, and also the negative value of ΔH indicates that the adsorption of superhalogens on $Mg_{12}O_{12}$ nanocage is exothermic.

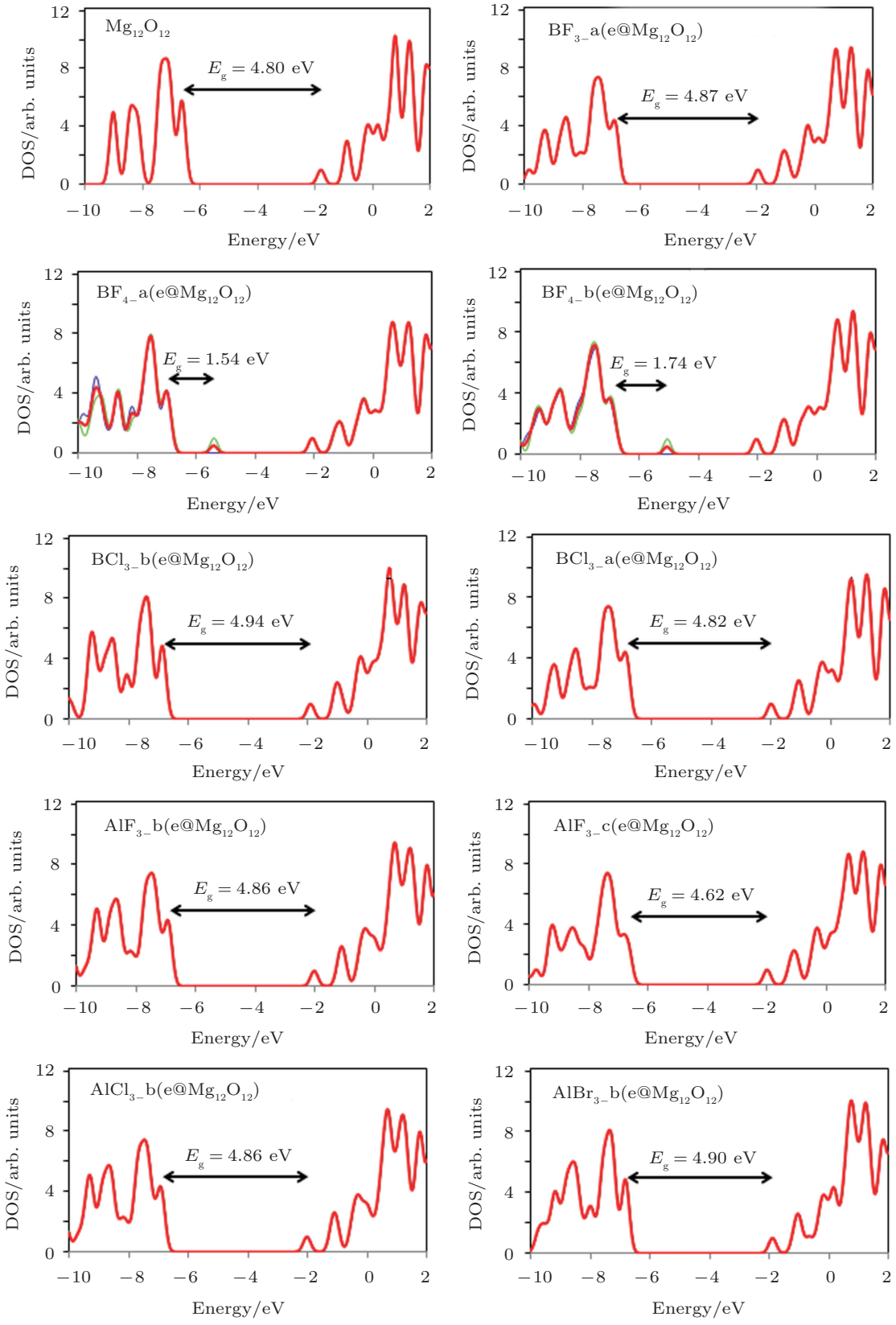
Table 1. Calculated values of energy gap E_g (in unit eV), the energy of the highest occupied molecular orbital E_{HOMO} (in unit eV), the energy of the lowest unoccupied molecular orbital E_{LUMO} (in unit eV), the binding energy E_b (in units kcal/mol), entropy change ΔS (in units cal/mol), free energy ΔG (in units kcal/mol), and enthalpy change ΔH (in units kcal/mol).

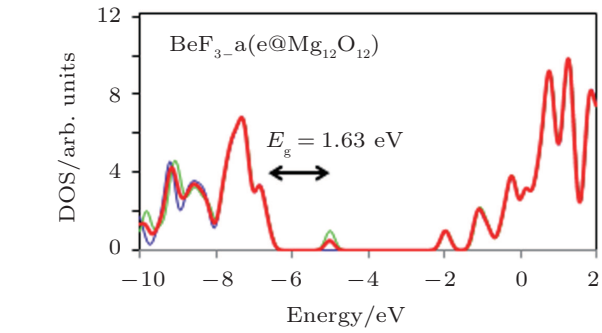
System	E_g	E_{HOMO}	E_{LUMO}	E_b	ΔH	ΔS	ΔG
Pristine	4.80	−6.58	−1.78	–	–	–	–
BF_3_a(e@$Mg_{12}O_{12}$)	4.87	−6.82	−1.95	−60.6	−61.2	−41.5	−48.8
BF_4_a(e@$Mg_{12}O_{12}$)	1.54	−6.93	−5.39	−96.0	−96.6	−45.7	−83.0
BF_4_b(e@$Mg_{12}O_{12}$)	1.74	−6.79	−5.05	−93.0	−93.6	−37.4	−82.4
BCl_3_b(e@$Mg_{12}O_{12}$)	4.94	−6.83	−1.89	−68.1	−68.7	−41.1	−56.4
AlF_3_a(e@$Mg_{12}O_{12}$)	4.82	−6.80	−1.98	−83.7	−84.3	−41.7	−71.8
AlF_3_b(e@$Mg_{12}O_{12}$)	4.77	−6.75	−1.98	−82.1	−82.7	−41.5	−70.3
AlF_3_c(e@$Mg_{12}O_{12}$)	4.62	−6.6	−1.98	−56.3	−56.9	−39.5	−45.2
$AlCl_3$_b(e@$Mg_{12}O_{12}$)	4.86	−6.87	−2.01	−75.8	−76.4	−39.9	−64.5
$AlBr_3$_b(e@$Mg_{12}O_{12}$)	4.9	−6.78	−1.88	−91.3	−91.8	−41.0	−79.6
BeF_3_a(e@$Mg_{12}O_{12}$)	1.83	−6.77	−4.94	−120.6	−121.2	−41.8	−108.7
BeF_3_b(e@$Mg_{12}O_{12}$)	0.96	−6.23	−5.27	−96.9	−97.5	−30.3	−88.5
BeF_3_c(e@$Mg_{12}O_{12}$)	0.96	−6.23	−5.27	−94.1	−94.7	−34.3	−84.4
GaF_3_a(e@$Mg_{12}O_{12}$)	4.8	−7.10	−2.30	−80.2	−80.8	−44.9	−67.4
GaF_3_b(e@$Mg_{12}O_{12}$)	4.65	−6.74	−2.09	−97.1	−97.7	−42.8	−85.0
GaF_3_c(e@$Mg_{12}O_{12}$)	4.77	−6.83	−2.06	−90.2	−90.8	−51.2	−75.5
$GaCl_3$_b(e@$Mg_{12}O_{12}$)	4.8	−6.84	−2.04	−76.7	−77.3	−40.1	−65.3
$GaCl_3$_c(e@$Mg_{12}O_{12}$)	4.83	−7.09	−2.26	−58.9	−59.5	−44.7	−46.1
$GaBr_3$_a(e@$Mg_{12}O_{12}$)	3.7	−5.96	−2.26	−143.8	−144.4	−37.0	−133.3
$GaBr_3$_b(e@$Mg_{12}O_{12}$)	3.23	−5.52	−2.29	−148.8	−149.3	−37.8	−138.1
NO_3_b(e@$Mg_{12}O_{12}$)	1.5	−6.82	−5.32	−35.4	−36.0	−40.4	−24.0
NO_3_c(e@$Mg_{12}O_{12}$)	1.97	−6.72	−4.75	−33.3	−33.9	−38.5	−22.4
BS_2_a(e@$Mg_{12}O_{12}$)	1.52	−6.63	−5.11	−17.6	−18.1	−32.9	−8.3
BS_2_ b(e@$Mg_{12}O_{12}$)	2.04	−6.75	−4.71	−64.3	−64.9	−36.1	−54.2
BSO_a(e@$Mg_{12}O_{12}$)	2.17	−6.72	−4.55	−68.5	−69.1	−38.0	−57.8
BO_2_ _a(e@$Mg_{12}O_{12}$)	1.73	−6.65	−4.92	−56.8	−57.3	−35.7	−46.7
BO_2_b(e@$Mg_{12}O_{12}$)	1.85	−6.61	−4.76	−55.6	−56.2	−34.2	−46.0
F_2_a(e@$Mg_{12}O_{12}$)	1.86	−6.59	−4.73	0.3	−0.3	−26.0	7.4
F_2_b(e@$Mg_{12}O_{12}$)	1.90	−6.59	−4.69	−0.2	−0.80	−30.0	8.1
PF_5_b(e@$Mg_{12}O_{12}$)	4.91	−6.89	−1.98	−69.7	−70.2	−42.0	−57.7
PCl_5_b(e@$Mg_{12}O_{12}$)	1.70	−6.45	−4.75	−4.2	−4.80	−26.1	3.0
PCl_5_c(e@$Mg_{12}O_{12}$)	2.49	−6.86	−4.37	−68.8	−69.4	−39.5	−57.6
AsF_5_b(e@$Mg_{12}O_{12}$)	4.41	−6.84	−2.43	−89.1	−89.7	−44.8	−76.3

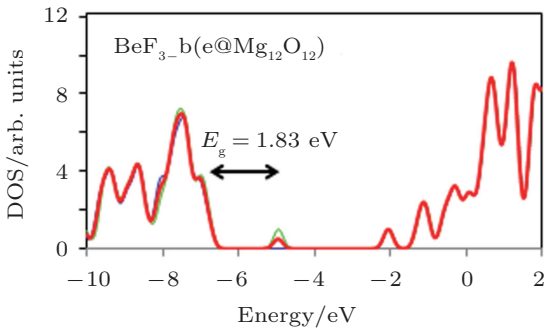
The values of ΔG^0 for F_2_a(e@$Mg_{12}O_{12}$), F_2_b(e@$Mg_{12}O_{12}$), and PCl_5_b(e@$Mg_{12}O_{12}$) are all positive and this can be explained with a small amount of binding energy (Table 1).

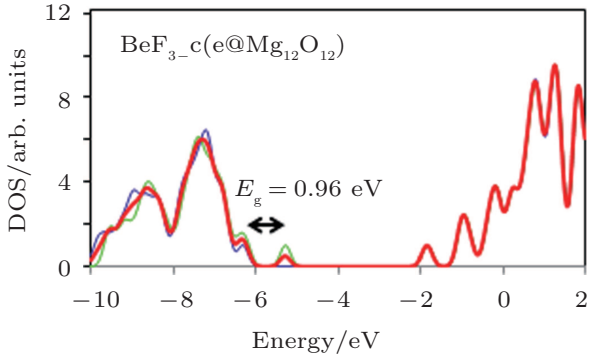
3.2. Electronic and optical property

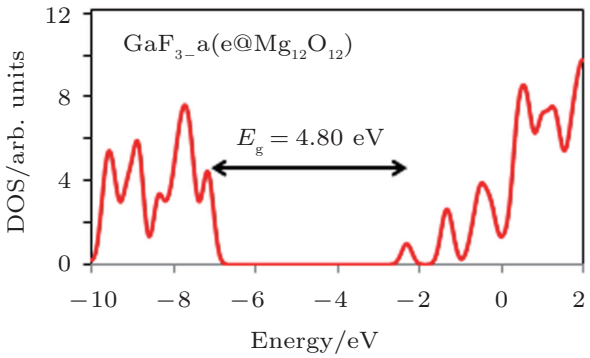
The values of energy gap E_g, which corresponds to the difference between the energy of the highest occupied molecular orbital (HOMO) and the energy of the lowest unoccupied molecular orbital (LUMO) are listed in Table 1. $Mg_{12}O_{12}$ nanocage is an intrinsic semiconductor with $E_g = 4.8$ eV. The plots of the calculated electronic densities of states (DOSs) for all mentioned structures are depicted in Fig. 3.

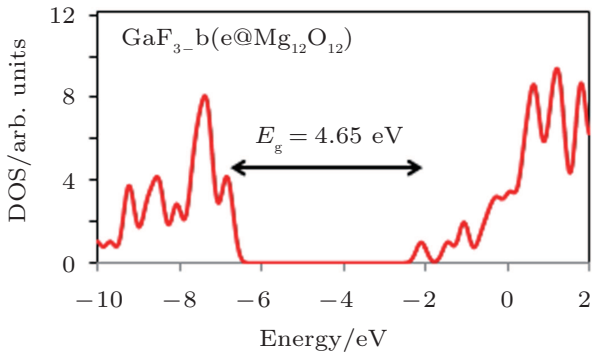


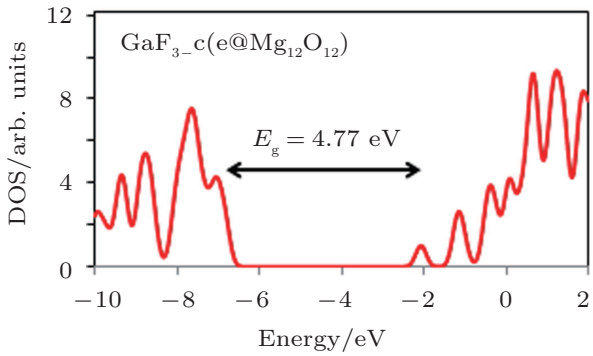

BeF3_a(e@Mg12O12)
Eg = 1.63 eV
DOS/arb. units
Energy/eV

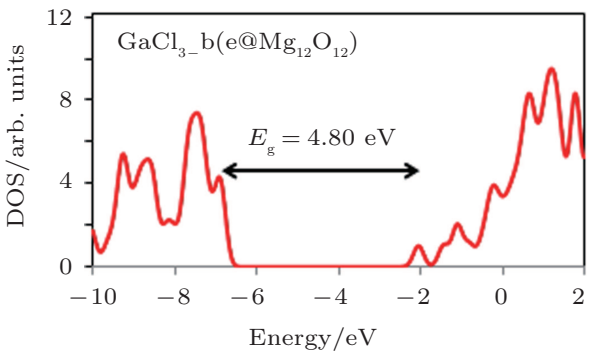

BeF3_b(e@Mg12O12)
Eg = 1.83 eV
DOS/arb. units
Energy/eV

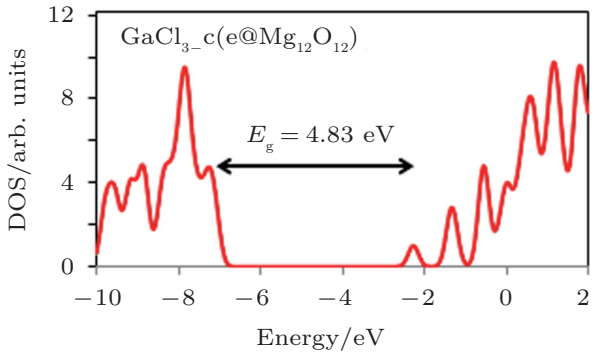

BeF3_c(e@Mg12O12)
Eg = 0.96 eV
DOS/arb. units
Energy/eV

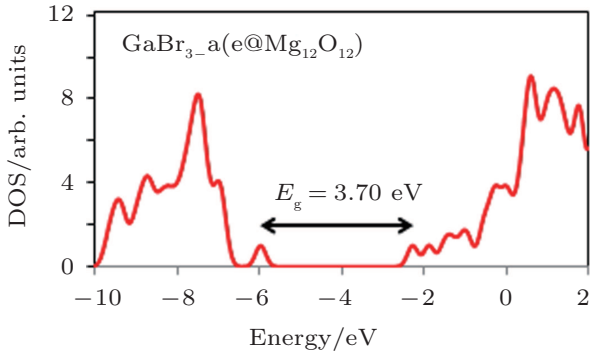

GaF3_a(e@Mg12O12)
Eg = 4.80 eV
DOS/arb. units
Energy/eV

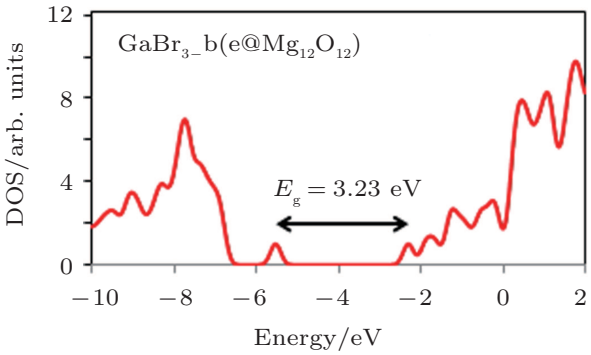

GaF3_b(e@Mg12O12)
Eg = 4.65 eV
DOS/arb. units
Energy/eV

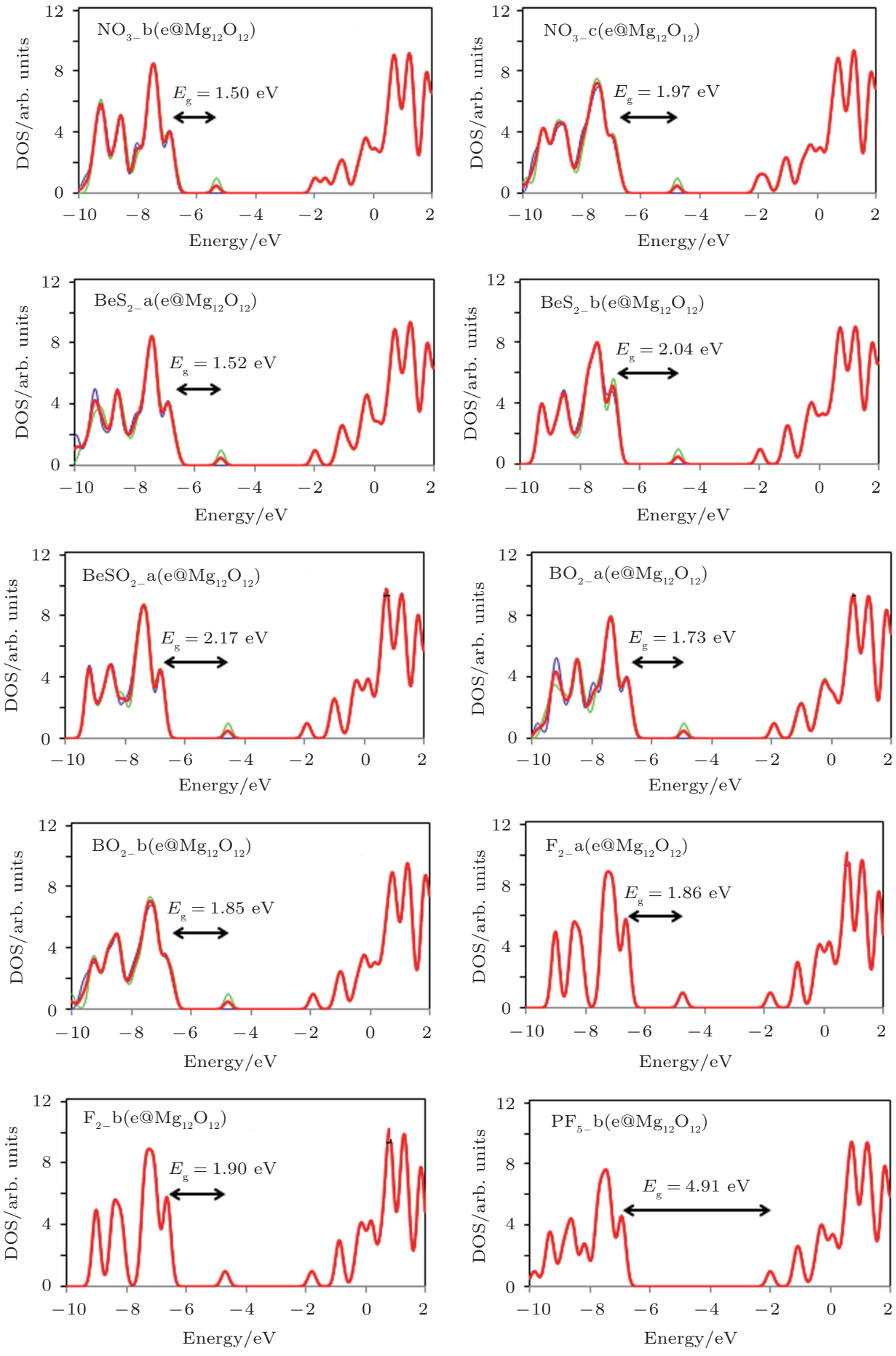

GaF3_c(e@Mg12O12)
Eg = 4.77 eV
DOS/arb. units
Energy/eV


GaCl3_b(e@Mg12O12)
Eg = 4.80 eV
DOS/arb. units
Energy/eV


GaCl3_c(e@Mg12O12)
Eg = 4.83 eV
DOS/arb. units
Energy/eV


GaBr3_a(e@Mg12O12)
Eg = 3.70 eV
DOS/arb. units
Energy/eV


GaBr3_b(e@Mg12O12)
Eg = 3.23 eV
DOS/arb. units
Energy/eV


NO3_b(e@Mg12O12)
Eg = 1.50 eV
NO3_c(e@Mg12O12)
Eg = 1.97 eV
BeS2_a(e@Mg12O12)
Eg = 1.52 eV
BeS2_b(e@Mg12O12)
Eg = 2.04 eV
BeSO2_a(e@Mg12O12)
Eg = 2.17 eV
BO2_a(e@Mg12O12)
Eg = 1.73 eV
BO2_b(e@Mg12O12)
Eg = 1.85 eV
F2_a(e@Mg12O12)
Eg = 1.86 eV
F2_b(e@Mg12O12)
Eg = 1.90 eV
PF5_b(e@Mg12O12)
Eg = 4.91 eV
DOS/arb. units
Energy/eV

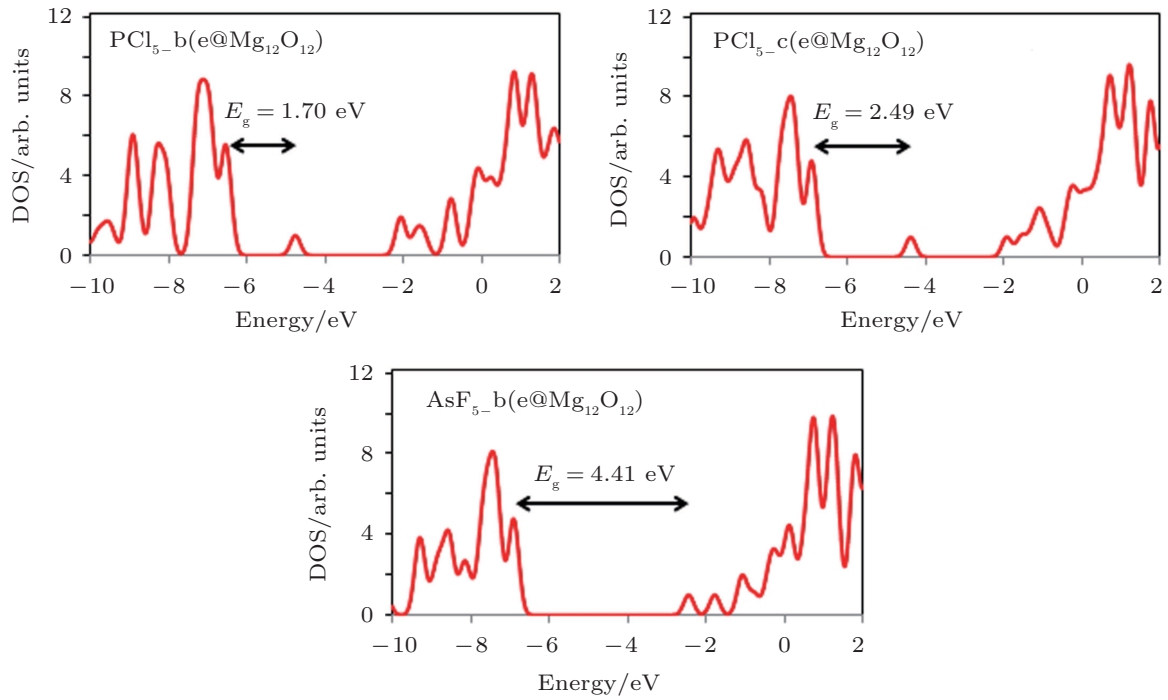


Fig. 3. (color online) Plots of the densities of states for $Mg_{12}O_{12}$ and XY_n(e@$Mg_{12}O_{12}$ (XY_n = BF_3, BF_4, BCl_3, AlF_3, $AlCl_3$, $AlBr_3$, BeF_3, GaF_3, $GaCl_3$, $GaBr_3$, NO_3, BS_2, BSO, BO_2, F_2, PF_5, PCl_5, and ASF_5). The red curve denotes the total DOS spectrum (scaled by 0.5), the blue curve represents the alpha DOS spectrum, and the green curve refers to the beta DOS spectrum. E_g is the energy gap.

In some structures, such as $GaBr_3$_a(e@$Mg_{12}O_{12}$) and $GaBr_3$_b(e@$Mg_{12}O_{12}$, the value of E_{HOMO} goes up while the E_{LUMO} is almost constant, so the value of energy gap E_g decreases. In some other structures, the main reason for E_g decreasing is the displacement of the E_{LUMO} energy downward and E_{HOMO} is almost constant. In some of these structures, E_g is constant. In Fig. 4, the variation trends of energy gap E_g, E_{HOMO}, and E_{LUMO} of all nanostructures are illustrated in Fig. 4.

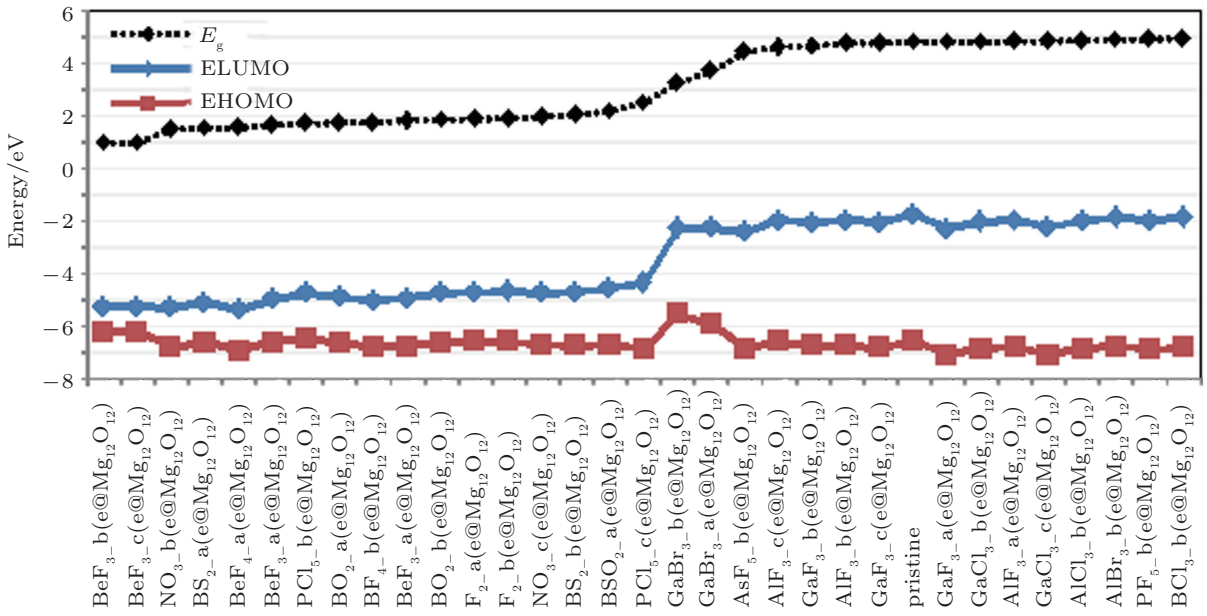


Fig. 4. (color online) Plots of E_g, E_{LUMO}, and E_{HOMO} for nanostructures based on $Mg_{12}O_{12}$.

Further, the values of dipole moment, polarizability, and hyperpolarizability for all above-mentioned structures are calculated by the CAM-B3LYP method. The values of the dipole moment, polarizability, and hyperpolarizability of nanostructures are presented in Table 2.

The results in Table 2 indicate that for all of the studied cases the dipole moment μ is considerably increased except for the systems F_2_a(e@$Mg_{12}O_{12}$) and F_2_b(e@$Mg_{12}O_{12}$) in which the values of μ are both nearly zero. This property can be explained with nearly zero charge on the F_2 molecule (Table 2).

Table 2. Values of permanent dipole moment μ (in unit a.u.), polarizability α (in unit a.u.), first hyperpolarizability β_0 (in unit a.u.), and q for the systems considered in this work.

System	μ	α	β_0	q
Pristine	0.00	215.4	0.2	–
BF_3_a(e@$Mg_{12}O_{12}$)	1.77	221.9	348.9	−0.335
BF_4_ a(e@$Mg_{12}O_{12}$)	2.78	257.8	312.6	−0.845
BF_4_b(e@$Mg_{12}O_{12}$)	2.67	242.1	4473.2	−0.833
BCl_3_b(e@$Mg_{12}O_{12}$)	1.59	259.5	506.6	−0.206
AlF_3_a(e@$Mg_{12}O_{12}$)	1.68	226.9	336.9	−0.069
AlF_3_b(e@$Mg_{12}O_{12}$)	1.76	227.1	347.4	−0.073
AlF_3_c(e@$Mg_{12}O_{12}$)	1.78	227.5	401.3	−0.077
$AlCl_3$_b(e@$Mg_{12}O_{12}$)	2.00	265.3	521.3	0.012
$AlBr_3$_b(e@$Mg_{12}O_{12}$)	1.14	289.5	433.2	0.095
BeF_3_a(e@$Mg_{12}O_{12}$)	2.49	233.2	2037.5	−0.939
BeF_3_b(e@$Mg_{12}O_{12}$)	2.87	242.0	4400.5	−0.825
BeF_3_c(e@$Mg_{12}O_{12}$)	1.44	315.0	5774.8	−0.806
GaF_3_a(e@$Mg_{12}O_{12}$)	4.37	230.5	644.0	−0.171
GaF_3_b(e@$Mg_{12}O_{12}$)	1.79	231.6	351.6	−0.098
GaF_3_c(e@$Mg_{12}O_{12}$)	2.78	225.9	551.2	−0.247
$GaCl_3$_b(e@$Mg_{12}O_{12}$)	1.83	271.2	476.4	−0.020
$GaCl_3$_c(e@$Mg_{12}O_{12}$)	4.20	270.3	842.0	−0.012
$GaBr_3$_a(e@$Mg_{12}O_{12}$)	2.63	315.4	641.5	−1.023
$GaBr_3$_b(e@$Mg_{12}O_{12}$)	5.19	308.4	1171.5	-1.041
NO_3_a(e@$Mg_{12}O_{12}$)	2.11	272.8	291.6	−0.804
NO_3_b(e@$Mg_{12}O_{12}$)	2.11	272.6	288.0	−0.0777
BS_2_ a(e@$Mg_{12}O_{12}$)	2.00	288.3	304.9	−0.648
BS_2_ b(e@$Mg_{12}O_{12}$)	2.10	289.1	937.8	−0.227
BSO_a(e@$Mg_{12}O_{12}$)	1.58	245.5	254.5	−0.335
BO_2_a(e@$Mg_{12}O_{12}$)	1.39	252.1	17.0	−0.818
BO_2_b(e@$Mg_{12}O_{12}$)	1.60	241.2	3935.9	−0.793
F_2_a(e@$Mg_{12}O_{12}$)	0.04	222.2	36.2	0.01
F_2_b(e@$Mg_{12}O_{12}$)	0.04	222.3	32.7	0.01
PF_5_b(e@$Mg_{12}O_{12}$)	2.07	231.4	423.7	−0.302
PCl_5_b(e@$Mg_{12}O_{12}$)	0.88	311.2	2780.5	0.099
PCl_5_c(e@$Mg_{12}O_{12}$)	1.84	301.5	512.2	−0.090
AsF_5_b(e@$Mg_{12}O_{12}$)	1.84	236.8	404.5	−0.161

The results in Table 2 show that by the adsorption of mentioned molecules on the $Mg_{12}O_{12}$ surface, in all cases, the polarizability value increases. Several trends are evident for polarizability in Table 2. First, the polarizability increases in the same configuration as $GaF_3(e@Mg_{12}O_{12}) > AlF_3(e@Mg_{12}O_{12}) > BF_3(e@Mg_{12}O_{12})$. This trend can be explained by the fact that in each group of the periodic table, the polarizability increases from top to bottom, the polarizability of the Ga atom is greater than those of Al and B. The polarizability increases in the same configuration as $AlBr_3(e@Mg_{12}O_{12}) > AlCl_3(e@Mg_{12}O_{12}) > AlF_3(e@Mg_{12}O_{12})$. Similarly, this trend can be explained as previously discussed (i.e., the amount of polarizability increases with the replacement of atoms in the lower row of the periodic table). Second, from left to right across a row of the periodic table, polarizability decreases ($BeF_3(e@Mg_{12}O_{12}) > BF_3(e@Mg_{12}O_{12})$).

Like polarizability, the results indicate that as a consequence of adsorption of all selected molecules on the $Mg_{12}O_{12}$ surface, the first hyperpolarizability value is increased. The quantities that β increases in these systems are very different, which depend on the type of adsorbing molecules and the adsorption geometry. It is clearly shown that the locations of the mentioned molecule adsorption on the $Mg_{12}O_{12}$ for all $XY_n(e@Mg_{12}O_{12})$ nanoclusters play an important role in increasing the calculated value of first hyperpolarizability (β_0). For example, first hyperpolarizability values of $BO_2(e@Mg_{12}O_{12})$ in a and b conformation are 17.0 a.u. and 3935.9 a.u., respectively.

4. Conclusions

In this work, we have studied the influences of adsorptions of some inorganic molecules on the electronic, optical, and thermodynamic properties of $Mg_{12}O_{12}$ nanocage by using the DFT method. The main results of this research can be summarized as follows.

(i) It is shown that almost all considered molecules each have an exothermic adsorption energy on the $Mg_{12}O_{12}$ surface.

(ii) The effects of XY_n molecules on the energy gap of the nanocage depend on the type of molecule and the position of adsorption.

(iii) For all studied systems, with the increase of adsorption of molecules the polarizability value increases.

(iv) The effects of adsorbing molecules on the polarizability depend on the type of molecule and the adsorption geometry, and it is shown that the polarizability increases in the same configuration as $GaF_3(e@Mg_{12}O_{12}) > AlF_3(e@Mg_{12}O_{12}) > BF_3(e@Mg_{12}O_{12})$ and increases for the similar structures as $BeF_3(e@Mg_{12}O_{12}) > BF_3(e@Mg_{12}O_{12}$.

(v) Additionally it is shown that the first hyperpolarizability value increases in each of all studied cases. Like the E_g and polarizability results, the value of the first hyperpolarizability depends on the type of adsorbing molecule and the adsorption geometry, however the sensitivity of hyperpolarizability to adsorption position is higher, and it is a key to estimating the value of increasing the first hyperpolarizability.

(vi) The large values of β_0 for the systems studied above suggest that these compounds may have potential applications in NLO materials.

References

[1] Sagadevan S and Varatharajan R 2013 *Materials Physics and Mechanics* **18** 11

[2] Wang Y, Xie X and Goodson T 2005 *Nano Lett.* **5** 2379
[3] Ji L L, Zhu B Q, Zhan T Y, Dai Y P, Zhu J, Ma W X and Lin Z Q 2011 *Acta Phys. Sin.* **60** 094210 (in Chinese)
[4] Reshak A H, Stys D, Auluck S and Kityk I V 2010 *J. Phys. Chem. B* **114** 18151
[5] Solomon R V, Veerapandian P, Vedha S A and Venuvanalingam P 2012 *J. Phys. Chem. A* **116** 4667
[6] Luo J, Haller M, Ma H, Liu S, Kim T D, Tian Y, Chen B, Jang S H, Dalton L R and Jen A K Y 2004 *J. Phys. Chem. B* **108** 8523
[7] Chen W, Li Z R, Wu D, Li Y, Sun C C and Gu F L 2005 *J. Am. Chem. Soc.* **127** 10977
[8] Wang W Y, Ma N N, Wang C H, Zhang M Y, Sun S L and Qiu Y Q 2014 *J. Mol. Graph Model.* **48** 28
[9] Qi H W, Sun Y X, Wang Z P, Zhang X Z, Yu F P, Sun X, Xu X G and Zhao X 2017 *Chin. Phys. B* **26** 084201
[10] Han W, Zhou L D, Xiang Y, Tian Y, Wang F, Li F Q, Wang L Q, Feng B, Zhao J P, Zheng K X, Zhu Q H, Wei X F, Zheng W G and Gong M L 2016 *Chin. Phys. Lett.* **33** 027803
[11] Ye T, Wei H, Hua Bao C, Fu Quan L, Bin F, Jun Pu Z, Kui Xing Z, Qi Hua Z and Wan G Z 2015 *Chin. Phys. Lett.* **32** 027801
[12] Zhang J J, Wang H F and Hou J H 2018 *Chin. Phys. B* **27** 034207
[13] Dong Z Z and Wei L S 2012 *Acta Phys. Sin.* **61** 064214 (in Chinese)
[14] Muhammad S, Janjua M R S A and Su Z 2009 *J. Phys. Chem. C* **113** 12551
[15] Mohammadi Hesari A, Shamlouei H R and Raoof Toosi A 2016 *J. Mol. Model.* **22** 189
[16] Shamlouei H R, Nouri A, Mohammadi A and Dadkhah Tehrani A 2016 *Physica E* **77** 48
[17] Omidi M, Shamlouei H R and Noormohammadbeigi M 2017 *J. Mol. Model.* **23** 82
[18] Noormohammadbeigi M and Shamlouei H R 2018 *J. Inorg. Organomet. Polym. Mater.* **28** 110
[19] Raoof Toosi A, Shamloue H Ri and Mohammadi Hesari A 2016 *Chin. Phys. B* **25** 094220
[20] Becke A D 1988 *Phys. Rev. A* **38** 3098
[21] Lee C, Yang W and Parr R G 1988 *Phys. Rev. B* **37** 785
[22] Frisch M J, *et al.*, Gaussian 09, revision A.1, Gaussian, Inc., 2009 Wallingford, CT
[23] Yanai T, Tew D P and Handy N C 2004 *Chem. Phys. Lett.* **393** 51
[24] Buckingham A D 1967 *Adv. Chem. Phys.* **12** 107
[25] McLean A D and Yoshimine M 1967 *J. Chem. Phys.* **47** 1927
[26] Thanthiriwatte K S and Silva K M N D 2002 *J. Mol. Struc. Thecochem.* **617** 169
[27] Wang J J, Zhou Z J, Bai Y, Liu Z B, Li Y, Wu D, Chen W, Li Z R and Sun C C 2012 *J. Mater. Chem.* **22** 24610
[28] Shakerzdeh E, Tahmasebi E and Shamlouei H R 2015 *SynthMet* **204** 17